

Bragg spectroscopy detection of quantum phases and excitation spectra of ultracold atoms in optical lattices

Jinwu Ye ¹, J.M. Zhang ², W.M. Liu ², Keye Zhang ³, Yan Li ³ and Weiping Zhang ³

¹ *Department of Physics, The Pennsylvania State University, University Park, PA, 16802, USA*

² *Institute of Physics, Chinese Academy of Sciences, Beijing, 100080, China*

³ *Department of Physics, East China Normal university, Shanghai, 200062, China*

(Dated: May 31, 2019)

Ultracold atoms loaded on optical lattices can provide unprecedented experimental systems for the quantum simulations and manipulations of many quantum phases and quantum phase transitions between these phases. However, so far, how to detect these quantum phases and phase transitions effectively remain an outstanding challenge. We show that Bragg spectroscopy of ultra-cold atoms loaded on optical lattices can be used to detect the ground states, the elementary excitation spectra and the corresponding spectral weights of many quantum phases. These phases include not only the well known superfluid and Mott insulating phases, but also other important phases such as charge density wave, valence bond solid and several kinds of supersolids and quantum phase transitions between these phases in one, two and three dimensional optical lattices.

Various kinds of strongly correlated quantum phases of matter may have wide applications in quantum information processing, storage and communications [1]. It was widely believed and also partially established that due to the tremendous tunability of all the parameters in this system, ultracold atoms loaded on optical lattices can provide an unprecedented experimental systems for the quantum simulations and manipulations of these quantum phases and quantum phase transitions between these phases. For example, Mott and superfluid phases [2] may have been successfully simulated and manipulated by ultra-cold atoms loaded in a cubic optical lattice [3]. However, there are at least two outstanding problems remaining. The first is to how to realize many important quantum phases [1]. The second is that assuming the favorable conditions to realize these quantum phases are indeed achieved in experiments, how to detect them without ambiguity. In this paper, we will address the second question. So far the experimental way to detect these quantum phases is mainly through the so called time of flight measurement [1, 3] which simply opens the trap and turn off the optical lattice and let the trapped atoms expand and interfere, then take the image. This kind of measurement is destructive. Further, it can not be used to measure the excitation spectrum. Another is through "Bragg spectroscopy" (BS) based on stimulated scattering of matter waves by laser pulses. The BS has been used to measure the excitation spectrum in both the particle excitation (high momentum) regime [4] and the collective excitation (low momentum) spectrum [5], also in strongly interacting ⁸⁵Rb at large scattering length across the Feshbach resonance [6]. Very recently, the momentum resolved Bragg spectroscopy [7] was used to probe the superfluid in optical lattices.

It remains an outstanding problem in ultra-cold atomic experiments to detect these quantum phases and quantum phase transitions without any ambiguity in a minimum destructive way. The Bragg spectroscopy in OL

could be considerably richer than that in a homogeneous gas inside a trap. In this paper, we will develop a systematic theory of using Bragg spectroscopy to detect the nature of quantum phases such as both the ground state and the excitation spectrum above the ground state of interacting bosons loaded in optical lattices. We explicitly show that the Bragg spectroscopy not only couple to the density order parameter, but also the *valence bond order* parameter due to the hopping of the bosons on the lattice. By tuning the angles between the two laser lights in Fig.1, the dynamic structure functions can detect not only the well known superfluid and Mott insulating phases, but also other interesting phases such as charge density wave (CDW) in Fig.2a,2c, valence bond solid (VBS) in Fig.2b,2d, CDW supersolid in Fig.1a and VBS supersolid in Fig.1b in all kinds of lattices [8–13]. It can also be used to measure the excitation spectrum and the corresponding spectral weights in all these phases shown in Fig.3. So the results to be achieved in this paper could be used in future experiments to detect all these conventional and exotic quantum phases as soon as these phases are within experimental reach. *In the following, we just take 2d optical lattices as examples. The 1d and 3d cases can be similarly discussed.*

The Boson Hubbard model with various kinds of interactions, on all kinds of lattices and at different filling factors is described by the following Hamiltonian [2, 8]:

$$\begin{aligned}
 H = & -t \sum_{\langle ij \rangle} (b_i^\dagger b_j + h.c.) - \mu \sum_i n_i + \frac{U}{2} \sum_i n_i (n_i - 1) \\
 & + V_1 \sum_{\langle ij \rangle} n_i n_j + V_2 \sum_{\langle ik \rangle} n_i n_k + \dots
 \end{aligned} \quad (1)$$

where $n_i = b_i^\dagger b_i$ is the boson density, t is the nearest neighbor hopping which can be tuned by the depth of the optical lattice potential, the U , V_1 , V_2 are onsite, nearest neighbor (nn) and next nearest neighbor (nnn) interactions respectively, the \dots may include further neigh-

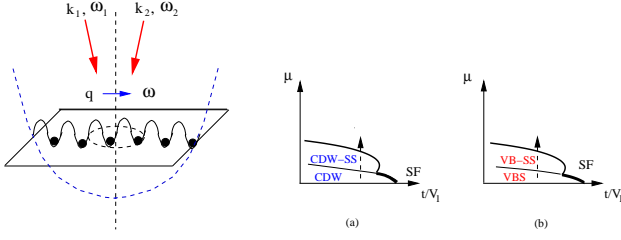


FIG. 1: Bragg spectroscopy of cold atoms moving in 2 dimensional optical lattices. The $\vec{q} = \vec{k}_1 - \vec{k}_2$ and $\omega = \omega_1 - \omega_2$ are momentum and energy transfer from the laser beams to the cold atoms respectively. Rotating the two laser beams around the dashed line can probe the excitation spectrum of the whole 2d optical lattice. Zero temperature Phase diagram [11] in (a) Ising limit. (b) Easy-Plane limit. The label of the axes are given in Eqn.1.

bor interactions and possible ring-exchange interactions. The filling factor $n = N/N_L$ where N is the number of atoms and $N_L = L^2$ is the number of lattice sites. The on-site interaction U can be tuned by the Feshbach resonance [2]. Various kinds of optical lattices such as a honeycomb or a triangular lattice [14], a body-centered-cubic lattice [14], a Kagome lattice [15] can be realized by suitably choosing the geometry of the laser beams forming the optical lattices. There are many possible ways to generate longer range interaction V_1, V_2, \dots of ultracold atoms loaded in optical lattices. Being magnetically or electrically polarized, the ^{52}Cr atoms [17] or polar molecules [18] $^{40}\text{K} + ^{87}\text{Rb}$ (or $^{39}\text{K} + ^{87}\text{Rb}$) interact with each other via long-rang anisotropic dipole-dipole interactions. Loading the ^{52}Cr or the polar molecules on a 2d optical lattice with the dipole moments perpendicular to the trapping plane can be mapped to Eqn.1 with long-range repulsive interactions $\sim p^2/r^3$ where p is the dipole moment. The CDW supersolid phases described in [11] by the dual vortex method was numerically found to be stable in large parameter regimes in this system [19]. Possible techniques to generate long-range interactions in a gas of groundstate alkali atoms by weakly admixing excited Rydberg states [20] with laser light was proposed in [21]. The generation of the ring exchange interaction has been discussed in [22]. Some of the important phases with long range interactions [8–13] are summarized in Fig.2.

The interaction between the two laser beams in Fig.1 with the two level bosonic atoms is:

$$H_{int} = \int d^2\vec{r} \Psi^\dagger(\vec{r}) \left[\frac{\vec{p}^2}{2m_a} + V_{OL}(\vec{r}) + \frac{\hbar\omega_a}{2} \sigma_z \right. \\ \left. + \frac{\Omega}{2} \sum_l (e^{-i\omega_l t} \sigma^+ u_l(\vec{r}) + h.c.) \right] \Psi(\vec{r}) \quad (2)$$

where $\Psi(\vec{r}) = (\psi_e, \psi_g)$ is the two component boson annihilation operator, the two Laser lights have frequencies ω_l and mode functions $u_l(\vec{r}) = e^{i\vec{k}_l \cdot \vec{r} + i\phi_l}$ in Fig.1. The Rabi

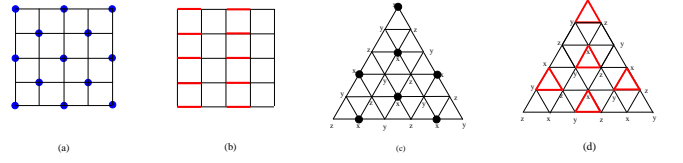


FIG. 2: The charge density wave (CDW) phase in a square lattice at $n_0 = 1/2$ with ordering wavevector $\vec{Q}_n = (\pi, \pi)$. (b) valence bond solid (VBS) phases in a square lattice at $n_0 = 1/2$ with ordering wavevector $\vec{Q}_K = (\pi, 0)$ where the kinetic energy $\langle K_{ij} \rangle = \langle b_i^\dagger b_j + h.c. \rangle$ takes a non-zero constant K in the two sites connected with a dimer, but 0 in the two sites without a dimer. (c) CDW at $\vec{Q}_n = (2\pi/3, 0)$ and (d) VBS at $\vec{Q}_K = (2\pi/3, 0)$ in triangular lattice at $n_0 = 1/3$. See [8–13].

frequencies Ω are much weaker than the laser beams (not shown in Fig.1) which form the optical lattices. When it is far off the resonance, the laser light-atom detunings $\Delta_l = \omega_l - \omega_a$ where ω_a is the two level energy difference are much larger than the Rabi frequency Ω . Because the energy transfer $\omega = \omega_1 - \omega_2$ is much smaller their detunings Δ_l , so $\Delta_1 \sim \Delta_2 = \Delta$. After adiabatically eliminating the upper level e of the two level atoms, expanding the ground state atom field operator $\psi_g(\vec{r}) = \sum_i b_i w(\vec{r} - \vec{r}_i)$ in Eqn.2 where $w(\vec{r} - \vec{r}_i)$ is the localized Wannier functions of the lowest Bloch band corresponding to $V_{OL}(\vec{r})$ and b_i is the annihilation operator of an atom at the site i , then we get the effective interaction between the off-resonant laser beams and the ground level g :

$$H_{int} = \hbar \frac{\Omega^2}{\Delta} \sum_{l,m} e^{-i(\omega_l - \omega_m)t} \left[\sum_i J_{i,i}^{lm} n_i + \sum_{\langle ij \rangle} J_{i,j}^{lm} b_i^\dagger b_j \right] \quad (3)$$

where the interacting matrix element is $J_{i,j}^{lm} = \int d\vec{r} w(\vec{r} - \vec{r}_i) u_l^*(\vec{r}) u_m(\vec{r}) w(\vec{r} - \vec{r}_j) = J_{j,i}^{lm}$. The first term in Eqn.3 is the onsite coupling. Because the Wannier wavefunction $w(\vec{r})$ can be taken as real in the lowest Bloch band, the second term can be written as $\hat{K} = \sum_{\langle ij \rangle} J_{i,j}^{lm} b_i^\dagger b_j = \sum_{\langle ij \rangle} J_{i,j}^{lm} (b_i^\dagger b_j + h.c.)$ which is nothing but the off-site coupling to the nearest neighbor kinetic energy of the bosons $K_{ij} = b_i^\dagger b_j + h.c.$. The intra-laser beam term $l = m$ only leads to a constant, So we only need to focus on the inter-laser beam terms $l \neq m$.

For the onsite coupling term, it is easy to show:

$$\hat{D}(\vec{q}) = f_0(\vec{q}) \sum_{i=1}^N e^{-i\vec{q} \cdot \vec{r}_i} n_i = f_0(\vec{q}) n(\vec{q}) \quad (4)$$

where $\vec{q} = \vec{k}_1 - \vec{k}_0$ and $f_0(\vec{q}) = \int d\vec{r} e^{-i\vec{q} \cdot \vec{r}} w^2(\vec{r})$ and $n(\vec{q}) = \sum_{\vec{k}} b_{\vec{k}}^\dagger b_{\vec{k}+\vec{q}}$ is the Fourier transform of the density operator at the momentum \vec{q} . In fact, more information is encoded in the off-site kinetic coupling in Eqn.3. In a square lattice, the bonds are either oriented along the \hat{x}

axis $\vec{r}_j - \vec{r}_i = \hat{x}$ or along the \hat{y} axis $\vec{r}_j - \vec{r}_i = \hat{y}$, we have:

$$\hat{K}_\square = f_x(\vec{q})K_x(\vec{q}) + f_y(\vec{q})K_y(\vec{q}) \quad (5)$$

where $K_\alpha(\vec{q}) = \sum_{i=1}^N e^{-i\vec{q}\cdot\vec{r}_i} K_{i,i+\alpha} = e^{iq_\alpha/2} \sum_{\vec{k}} \cos k_\alpha b_k^\dagger b_{\vec{k}+\vec{q}}$ are the Fourier transform of the kinetic energy operator $K_{ij} = b_i^\dagger b_j + h.c.$ along $\alpha = x, y$ bonds at the momentum \vec{q} and the "form" factors $f(\vec{q}, \vec{r}_i - \vec{r}_j) = \int d\vec{r} e^{-i\vec{q}\cdot\vec{r}} w(\vec{r}) w(\vec{r} + \vec{r}_i - \vec{r}_j)$. In general, $f_\alpha/f_0 \sim 0.1$.

The response function of the cold atom systems to the perturbation Eqn.3 can be calculated by using the standard linear response theory:

$$S(\vec{q}, \omega) = \left(\frac{\Omega^2}{\Delta}\right)^2 [|f_0(\vec{q})|^2 S_n(\vec{q}, \omega) + \sum_{\alpha=\hat{x}, \hat{y}} |f_\alpha(\vec{q})|^2 S_{K_\alpha}(\vec{q}, \omega)] \quad (6)$$

where $\vec{q} = \vec{k}_1 - \vec{k}_0, \omega = \omega_1 - \omega_2$, the $S_n(\vec{q}, \omega) = \langle n(-\vec{q}, -\omega) n(\vec{q}, \omega) \rangle$ is the dynamic density-density response function whose Lehmann representation was listed in [5]. The $S_{K_\alpha}(\vec{q}, \omega) = \langle K_\alpha(-\vec{q}, -\omega) K_\alpha(\vec{q}, \omega) \rangle$ is the bond-bond response function whose Lehmann representation can be got from that of the $S_n(\vec{q}, \omega)$ simply by replacing the density operator $n(\vec{q})$ by the bond operator $K_\alpha(\vec{q})$. The *equal-time* response function is $S(\vec{q}) = \int d\omega S(\vec{q}, \omega) = 2\pi \left(\frac{\Omega^2}{\Delta}\right)^2 [|f_0(\vec{q})|^2 S_n(\vec{q}) + \sum_{\alpha=\hat{x}, \hat{y}} |f_\alpha(\vec{q})|^2 S_{K_\alpha}(\vec{q})]$. In the following, we will discuss the physical implications of Eqn.6 on phase diagram Fig.1.

At the 1/2 filling along the horizontal axis in Fig.1a, inside the SF state near the CDW, there is a peak of $S_n(\vec{q})$ near $\vec{Q}_n = (\pi, \pi)$, so the SF to the CDW transition is a first order one driven by the instability of the peak. Due to the lack of VBS order on both sides, the second term in Eqn.6 can be neglected, so that

$$S_{CDW}(\vec{q}, \omega) \sim \left(\frac{\Omega^2}{\Delta}\right)^2 |f_0(\vec{q})|^2 S_n(\vec{q}, \omega) \quad (7)$$

When one gets into the CDW state at \vec{Q}_n in Fig.1a, then the $S_n(\vec{q})$ should show a peak near $\vec{q} = \vec{Q}_n$ whose amplitude scales as the number of atoms inside the trap $\sim |f_0(\pi, \pi)|^2 N \sim |f_0(\pi, \pi)|^2 L^2 \times n_0$. Slightly away from 1/2 filling, the transition from the CDW to the CDW-SS along the vertical axis in Fig.1a near $\vec{q} = (0, 0)$ is shown [11] to be in the same universality class of SF to Mott transition [2] with the critical exponents $z = 2, \nu = 1/2, \eta = 0$ upto a logarithmic correction [11]. We have $\langle n(\vec{q}) \rangle = n_0 \delta_{\vec{q}, \vec{Q}_n} + \delta n \delta_{\vec{q}, 0}$ where $n_0 = 1/2$ in *both* the CDW and the CDW+SS and $\delta n = n - 1/2$. Using the result in [25], one can see that $\delta n = \frac{m_a \mu a^2}{4\pi \hbar^2} \ln\left[\frac{\hbar^2}{2m_a \mu a^2}\right]$ at $T = 0$. From the scaling analysis in [25], because δn is a conserved quantity, so it has no anomalous dimension, one can show that when q is not too close to the Brillouin Zone boundary,

$S_n(\vec{q}, \omega) = \frac{2m_a^4}{\hbar^2} \Phi_n\left(\frac{\hbar\omega}{k_B T}, \frac{\hbar q}{\sqrt{2m_a k_B T}}, \frac{\mu}{k_B T}\right)$ upto a logarithmic factor where Φ_n is a universal function independent of the atom-atom interactions in Eqn.1. Inside the CDW-SS phase in Fig.1a, there should also be a $S_n(\vec{q})$ peak $\sim |f_0|^2 L^2 \times n_0 < |f_0|^2 L^2 \times n$ at $\vec{q} = \vec{Q}_n$ signaling its CDW order.

At the 1/2 filling along the horizontal axis in Fig.1b, inside the SF state near the VBS, there is a peak of $S_K(\vec{q})$ near $\vec{Q}_K = (\pi, 0)$, so the SF to the VBS transition is a very weak first order one [26], namely, weaker than the SF-CDW transition by a factor of $|f_x/f_0|^2 \sim 10^{-2}$. When one gets into the VBS state at \vec{Q}_K in Fig.1b, the first term leads to much higher energy excitations, so the second term in Eqn.6 dominates over the first term in the low energy sector, then

$$S_{VBS}(\vec{q}, \omega) \sim \left(\frac{\Omega^2}{\Delta}\right)^2 \sum_{\alpha=\hat{x}, \hat{y}} |f_\alpha(\vec{q})|^2 S_{K_\alpha}(\vec{q}, \omega) \quad (8)$$

where the $S_K(\vec{q})$ should show a peak at $\vec{q} = \vec{Q}_K$ signifying the VBS ordering at \vec{Q}_K whose amplitude scales as the number of atoms inside the trap $\sim |f_x|^2 N \sim |f_x|^2 L^2 \times n_0$. So the rate of divergence of a VBS order as L gets to large is $|f_x/f_0|^2 \sim 10^{-2}$ times smaller than that of a CDW order. Slightly away from 1/2 filling, the transition from the VBS to the VB-SS along the vertical axis in Fig.1b near $\vec{q} = (0, 0)$ is also shown to be in the same universality class of SF to Mott transition with the critical exponents $z = 2, \nu = 1/2, \eta = 0$ upto a logarithmic correction [11]. We have $\langle \hat{K}_\square(\vec{q}) \rangle = f_x(\vec{Q}_K) K \delta_{\vec{q}, \vec{Q}_K}$ and $\langle n(\vec{q}) \rangle = (\delta n + 1/2) \delta_{\vec{q}, 0}$ where $\delta n = n - 1/2$. In the VB-SS phase in Fig.1b, there should also be a $S_K(\vec{q})$ peak $\sim |f_x|^2 L^2 \times n_0 < |f_x|^2 L^2 \times n$ at $\vec{q} = \vec{Q}_K = (\pi, 0)$ due to the valence bond ordering at \vec{Q}_K . Note the separation of momentum scale of VBS order at $\vec{q} = \vec{Q}_K = (\pi, 0)$ and the SF order near $\vec{q} = 0$. Both can be easily distinguished by tuning the difference between \vec{k}_1 and \vec{k}_0 through changing the two relative angles of the two laser beams in Fig.1.

So far, we only discussed the ground state properties of various quantum states. The elementary excitation spectrum above these ground states can be determined from the peak positions of the corresponding dynamic density-density or bond-bond response functions. Eqn.6 shows that the response function of the cold atom system is the sum of the two response functions with the corresponding spectral weight $|f_0|^2$ and $|f_\alpha|^2$. The $\langle \delta n \delta n \rangle$ correlation function inside a SF was studied in several different physical systems in [23, 24]. It was found that $S_n(\vec{q}, \omega) = S_n(\vec{q}) \delta(\omega - \omega(q))$ where $S_n(\vec{q}) = \rho_s q^2 \pi / 2\omega(q)$ is the equal time density-density correlation function, $\omega(q) = \rho_s q^2 (\alpha - \beta q^2 + \gamma q^4)$ with $\alpha, \beta, \gamma > 0$ is the superfluid phonon spectrum shown in Fig.3a1, the ρ_s and $\kappa = 1/\alpha$ are the superfluid density and the compressibility respectively. *Up to a reciprocal lattice vector*, the wavevector is confined to $L^{-1} < q < a^{-1}$ where the trap

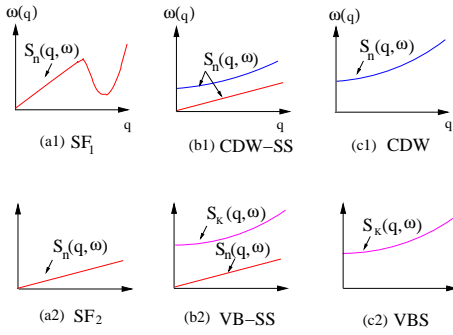


FIG. 3: The excitations spectrum (not too close to the Brillouin Zone boundary) in the CDW, VBS, SF, CDW-SS and VB-SS states which are the peak positions of the corresponding dynamic response functions shown with arrows. The corresponding spectral weights are worked out in the text.

size $L \sim 100\mu m$ and the lattice constant $a \sim 0.5\mu m$ in Fig.1. In the SF near to the CDW, there is a roton minimum near \vec{Q}_n , the $S_n(\vec{q})$ shows a peak near \vec{Q}_n . Inside the CDW-SS, the roton minimum disappears and is replaced the upper branch with a CDW gap and a spectral weight $\sim n_0 = 1/2$ in the Fig.3b1, the lower superfluid branch in the Fig.3b1 has a spectral weight $\sim \rho_s \sim \delta n = n - 1/2$. Inside the CDW, the superfluid lower branch disappears, the upper CDW branch in Fig.3c1 has the spectral weight $n = n_0 = 1/2$.

In the SF near to the VB, there is no peak in $S_n(\vec{q})$, so there is no corresponding roton minimum near \vec{Q}_K as shown in the Fig.3a2. However, $S_K(\vec{q})$ shows a peak near \vec{Q}_K which is suppressed by a factor $|f_x|^2$ as shown in Eqn.6. Inside the VB-SS, the SF order of the VB-SS encoded in the $\langle \delta n \delta n \rangle$ correlation function is the same as the SF inside the CDW-SS. So there is a upper branch with a VBS gap and a spectral weight $|f_x|^2 \times n_0$ in the Fig.3b2, also a lower superfluid branch in the Fig.3b2 with the spectral weight $|f_0|^2 \times \delta n$. So when $\delta n \sim |f_x/f_0|^2 n_0 \sim 10^{-2} n_0$, the two spectral weights become comparable. Inside the VBS, the superfluid lower branch disappears, the upper VBS branch has the spectral weight $|f_x|^2 \sim n = n_0 = 1/2$. The elementary excitation spectra of all the possible quantum phases with the corresponding spectral weight are shown in Fig.3

The procedures discussed in the square lattice can be generalized to other lattices such as the honeycomb, triangular and kagome lattices. For all the three lattices, there are three different orientations of bonds aligned along $\hat{a}, \hat{b}, \hat{c}$. Taking the triangular lattice which is also a Bravais lattice in Fig.2c,2d for example, Eqn.5 should be generalized to:

$$\hat{K}_\Delta = f_a(\vec{q})K_a(\vec{q}) + f_b(\vec{q})K_b(\vec{q}) + f_c(\vec{q})K_c(\vec{q}) \quad (9)$$

where $\vec{q} = \vec{k}_1 - \vec{k}_0$. For the $\vec{Q}_K = (2\pi/3, 0)$ ordering of the Triangular valence bond in Fig.2d, $K_a = K_b = K_c$. The generalization to non-Bravais lattices such the honey-

comb, Kagome, Sutherland-Shastry and checkboard lattices [12, 16] can also be worked out similarly. The effects of the trap and finite temperature will be discussed in a future work.

We thank G.G. Batrouni, Jason Ho, S. V. Isakov, Jing Zhang and Tiancai Zhang for helpful discussions. JYE's research at KITP-C is supported by the Project of Knowledge Innovation Program (PKIP) of Chinese Academy of Sciences. W.M. Liu's research was supported by NSFC under grants No. 10874235, the NKBRSCF under Grants Nos. 2006CB921400 and 2009CB930700. W.P. Zhang's research was supported by the National Natural Science Foundation of China under Grants No. 10588402 and No. 10474055, the National Basic Research Program of China (973 Program) under Grant No. 2006CB921104, the Program of Shanghai Subject Chief Scientist under Grant No. 08XD14017, the Program for Changjiang Scholars and Innovative Research Team in University.

-
- [1] For a review, see M. Lewenstein, *et al*, Adv. Phys. 56, 243-379 (2007). I. Bloch, J. Dalibard, W. Zwerger, Rev. Mod. Phys. 80, 885 (2008).
 - [2] D. Jaksch, C. Bruder, J. I. Cirac, C. W. Gardiner, and P. Zoller, Phys. Rev. Lett. 81, 3108 - 3111 (1998).
 - [3] M. Greiner, *et al*, Nature 415, 39-44 (2002).
 - [4] J. Stenger *et al.*, Phys. Rev. Lett. 82, 4569 (1999);
 - [5] D. M. Stamper-Kurn *et al*, Phys. Rev. Lett. 83, 2876 - 2879 (1999).
 - [6] S. B. Papp, *et.al*, Phys. Rev. Lett. 101, 135301 (2008).
 - [7] P. T. Ernst, *et al*, Nature Physics 6, 56 (2010).
 - [8] G. Murthy, D. Arovas, A. Auerbach, Phys. Rev. B 55, 3104-3121 (1997).
 - [9] F. Hbert *et.al*, Phys. Rev. B 65, 014513 (2001), P. Sengupta, *et.al*, Phys. Rev. Lett. 94, 207202 (2005). G.G. Batrouni, F. Hebert, R.T. Scalettar, Phys. Rev. Lett. 97, 087209 (2006).
 - [10] Longhua Jiang and Jinwu Ye, J. Phys, Condensed Matter. 18 (2006) 6907-6922
 - [11] Jinwu Ye, Nucl. Phys. B 805 (3) 418-440 (2008).
 - [12] Yan Chen and Jinwu Ye, preprint submitted to Nucl. Phys.B.
 - [13] Jing Yu Gan, Yu Chuan Wen, Jinwu Ye, Tao Li, Shi-Jie Yang, Yue Yu, Phys. Rev. B 75, 214509 (2007).
 - [14] G. Grynberg, *et al*, Phys. Rev. Lett. 70, 2249 -2252 (1993).
 - [15] L. Santos, *et.al*, Phys. Rev. Lett. 93, 030601 (2004). B. Damski, *et.al*, Phys. Rev. A 72, 053612 (2005).
 - [16] For a review, see C. Lhuillier and G. Misguich, arXiv:cond-mat/0109146
 - [17] A. Griesmaier, *et.al*, Phys. Rev. Lett. 94, 160401 (2005)
 - [18] K.-K. Ni, *et al*, Science 322, 231 (2008).
 - [19] B. Capogrosso-Sansone, *et al*, arXiv:0906.2009.
 - [20] E. Urban *et al*, Nat. Phys, in press; A. Gaetan. *et al*, Nat. Phys. in press. Jan.2009
 - [21] G. Pupillo, *et al*, arXiv:1001.0519.
 - [22] H. P. Bchler, *et.al*, Phys. Rev. Lett. 95, 040402 (2005).
 - [23] Jinwu Ye, Phys. Rev. Lett. 97, 125302 (2006); Euro-

- physics Letters, 82 (2008) 16001; cond-mat/0603269. Due to the lattice phonon of the elastic lattice, the excitation spectrum inside the continuous supersolid was called 'supersolidon' which also has an upper and a lower branch, both of which are gapless, so quite different than the spectrum inside the CDW-SS shown in Fig.3b1.
- [24] Jinwu Ye and Longhua Jiang, Phys. Rev. Lett. 98, 236802 (2007); Jinwu Ye, Phys. Rev. Lett. 97, 236803 (2006), Annals of Physics, 323 (2008), 580-630, arXiv:0712.0437 to appear in Jour. of Low Temp. Phys.
- [25] Subir Sachdev, T. Senthil, and R. Shankar, Phys. Rev. B 50, 258 (1994); A. Chubukov, S. Sachdev and Jinwu Ye, Phys.Rev.B, 11919 (1994).
- [26] This intuitive physical picture is consistent with the first order scenario from QMC by A. Kuklov *et.al*, cond-mat/0602466; in contrast to the deconfined quantum critical scenario by T. Senthil *et.al*, Science 303, 1490 (2004).